Supporting Information for:

A New Nitrogen Fixation Strategy: Direct Formation of $^{*}N_2^{-}$ Excited State on Metal-Free Photocatalyst

Xianghong Niu,[1] Dazhong Sun, [1] Li Shi,[2] Xiaowan Bai,[2] Qiang Li,[2] Xing'ao Li,[1,3] Jinlan Wang[2*]

[1] New Energy Technology Engineering Laboratory of Jiangsu Province & School of Science, Nanjing University of Posts and Telecommunications (NJUPT), Nanjing 210023, China

[2] School of Physics, Southeast University, Nanjing 211189, China

[3] Key Laboratory for Organic Electronics and Information Displays & Institute of Advanced Materials (IAM), Jiangsu National Synergistic Innovation Center for Advanced Materials (SICAM), Nanjing University of Posts & Telecommunications, Nanjing 210023, China

E-mail: *jlwang@seu.edu.cn (J.W.);

Nonadiabatic molecular dynamics

The system temperature is firstly brought to 300 K utilizing the repeated velocity rescaling method based on the optimizing geometry at 0K using VASP. Next, a 8 ps microcanonical *ab initio* molecular dynamics (MD) trajectory and wave function were generated with a time step of 1 fs. Finally, the nonadiabatic molecular dynamics (NAMD) results were obtained via averaging over the 100 different initial configurations from the *ab initio* MD trajectory using Hefei-NAMD code. For each chosen initial configurations, we sampled 2×10^3 trajectories for the next 5 ps. The quantum-classical decoherenceinduced surface hopping (DISH) algorithm was employed to provide a probability for hopping between interacting states using the evolution of the adiabatic (AD) basis coefficients.[1, 2]

The geometric structures of excited state from time-dependent density functional theory (TDDFT)

The TDDFT computations were carried out using Becke three-parameter Lee-Yang-Parr hybrid [3] exchange-correlation functional along with the Slater-type double-zeta plus polarization basis set [4] implemented in the Amsterdam Density Functional program package.[5-7] The ground state geometries of nanoparticals were first optimized at DFT level. Then, based on the ground state structure, the geometric structures of excited state were calculated using TDDFT. The lowest excited state were taken into consideration since high excited states rapidly relaxed to the lowest excited state according to Kasha's rule. All optimizations were done without any symmetry constraint.

Free Energy Calculations

The calculations of Gibbs free energy change (ΔG) for each elemental step was based on the computational hydrogen electrode model proposed by NørsÅkov et al.,[8] which can be computed by:

$$\Delta G = \Delta E + \Delta E_{ZPE} - T\Delta S$$

where ΔE is the electronic energy difference between the initial and adsorption states of reaction intermediates; ΔE_{ZPE} and ΔS are the changes in zero point energies and entropy, respectively. T is the temperature, which is set to be 298.15 K in this work. The ΔE_{ZPE} can be acquired through vibrational frequency calculation. The chemical potential (μ) of a proton-electron pair is equal to half of the chemical potential of gaseous hydrogen: $\mu_{H^+} + \mu_{e^-} = \frac{1}{2}\mu_{H_2}$.

Optical absorption spectrum

Heyd-Scuseria-Ernzerhof (HSE06) hybrid functional was adopted to probe into the optical absorption properties by calculating the dielectric constants [9] using Vienna ab initio Simulation Package (VASP)

$$\varepsilon_{\alpha\beta}^{(2)}(\omega) = \frac{4\pi^2 e^2}{\Omega} \lim_{q\to 0} \frac{1}{q^2} \sum_{c,v,\mathbf{k}} 2w_{\mathbf{k}} \delta(\varepsilon_{c\mathbf{k}} - \varepsilon_{v\mathbf{k}} - \omega) \times \left\langle u_{c\mathbf{k}+e_\alpha \mathbf{q}} \mid u_{v\mathbf{k}} \right\rangle \left\langle u_{c\mathbf{k}+e_\beta \mathbf{q}} \mid u_{v\mathbf{k}} \right\rangle *$$

Where Ω is the volume of the primitive cell, q is the electron momentum operator, c and v are the conduction and valence band states, respectively, $\omega_{\mathbf{k}}$ is the **k** point weight, $\varepsilon_{c\mathbf{k}}$, $\varepsilon_{v\mathbf{k}}$ and $\mu_{c\mathbf{k}}$, $\mu_{v\mathbf{k}}$ are the eigenvalues and wave-functions at the **k** point, respectively, and e_α, e_β are the unit vectors for the three Cartesian directions.

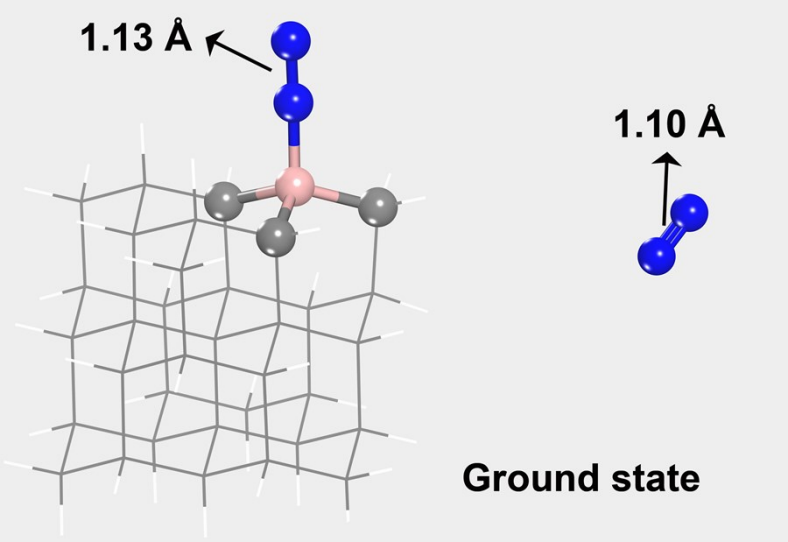

Figure S1. The optimized geometric structure of N_2 adsorbing on BDC and free N_2. The bond length of N_2 adsorbing on BDC and free N_2 is 1.13 and 1.10 Å, respectively. The grey, pink and blue balls indicate the carbon, boron and nitrogen, respectively. The grey and white line denote the carbon and hydrogen, respectively.

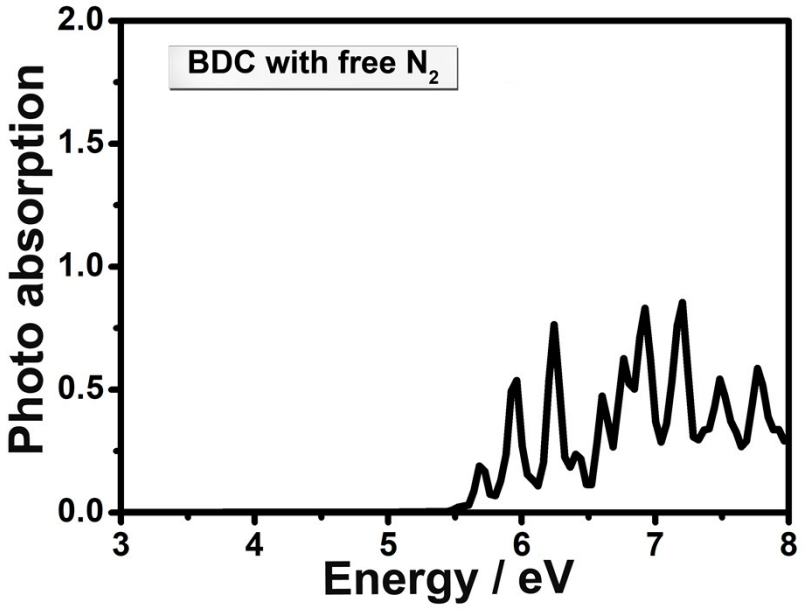

Figure S2. Photoabsorption performance of BDC with free N_2. The incident light polarized along with the *x* direction.

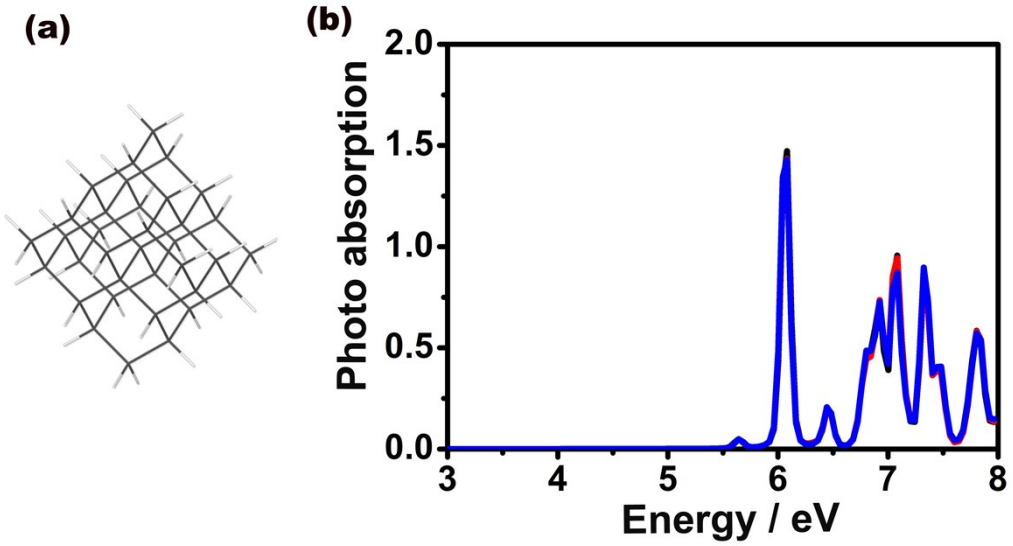

Figure S3. The (a) geometric structure and (b) photoabsorption performance of pristine DC. The grey and white lines in (a) denote the carbon and hydrogen, respectively. The black, red and blue lines in (b) denote the light absorption region for the incident light polarized along with the x, y and z directions, respectively.

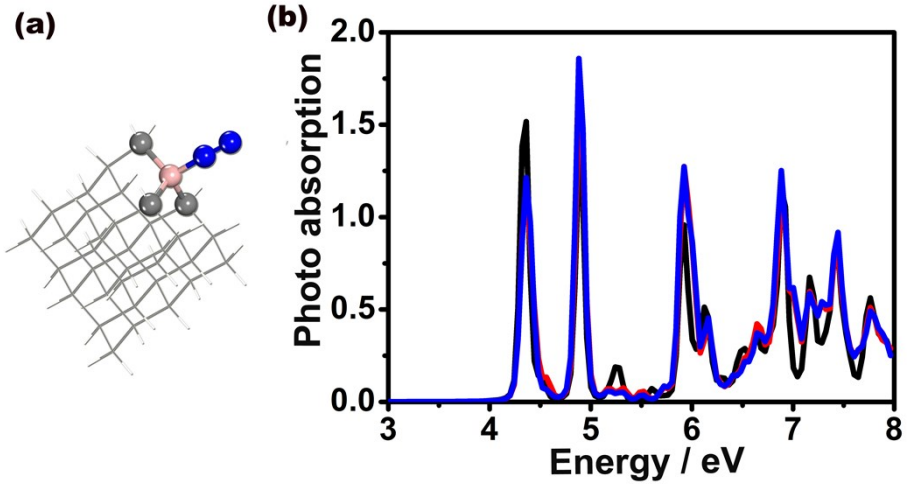

Figure S4. The (a) geometric structure and (b) photoabsorption performance of BDC adsorbing N_2 ligand. The grey, pink and blue balls in (a) indicate the carbon, boron and nitrogen, respectively. The grey and white lines in (a) denote the carbon and hydrogen, respectively. The black, red and blue lines in (b) denote the light absorption region for the incident light polarized along with the x, y and z directions, respectively.

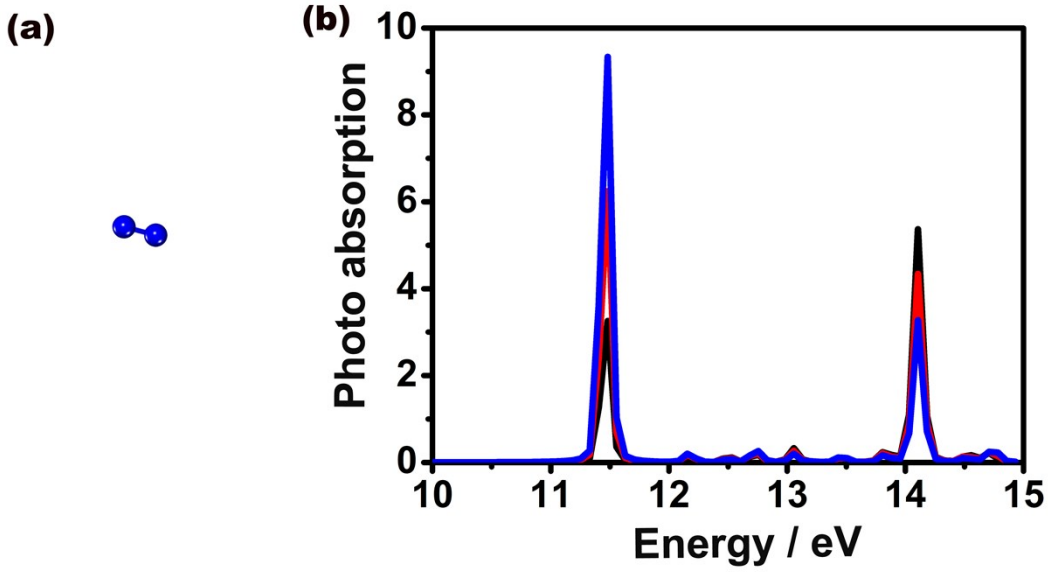

Figure S5. The (a) geometric structure and (b) photoabsorption performance of free N_2. The blue balls in (a) indicate the nitrogen. The black, red and blue lines in (b) denote the light absorption region for the incident light polarized along with the x, y and z directions, respectively.

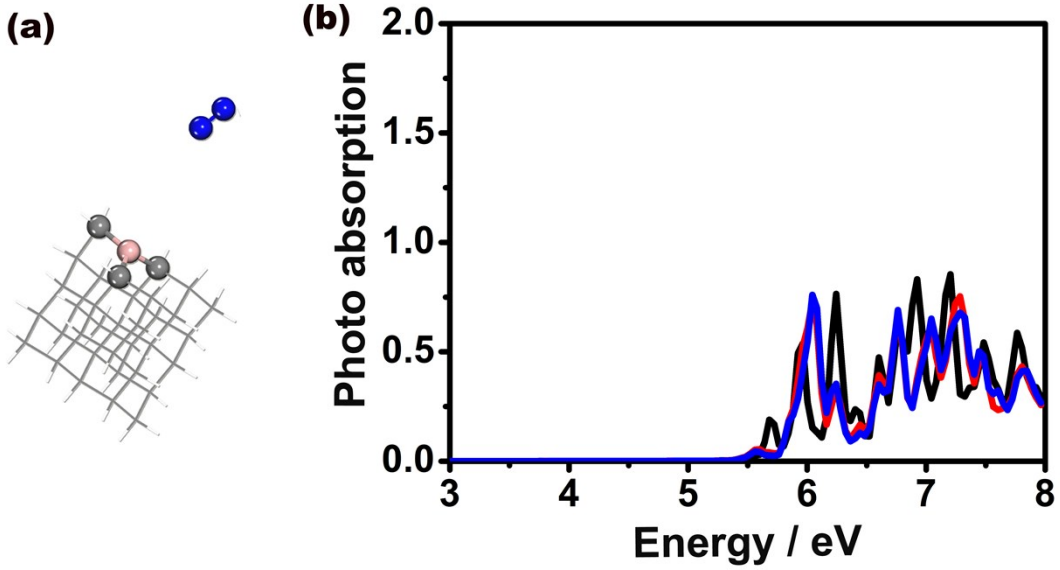

Figure S6. The (a) geometric structure and (b) photoabsorption performance of BDC with free N_2. The grey, pink and blue balls in (a) indicate the carbon, boron and nitrogen, respectively. The grey and white lines in (a) denote the carbon and hydrogen, respectively. The black, red and blue lines in (b) denote the light absorption region for the incident light polarized along with the x, y and z directions, respectively.

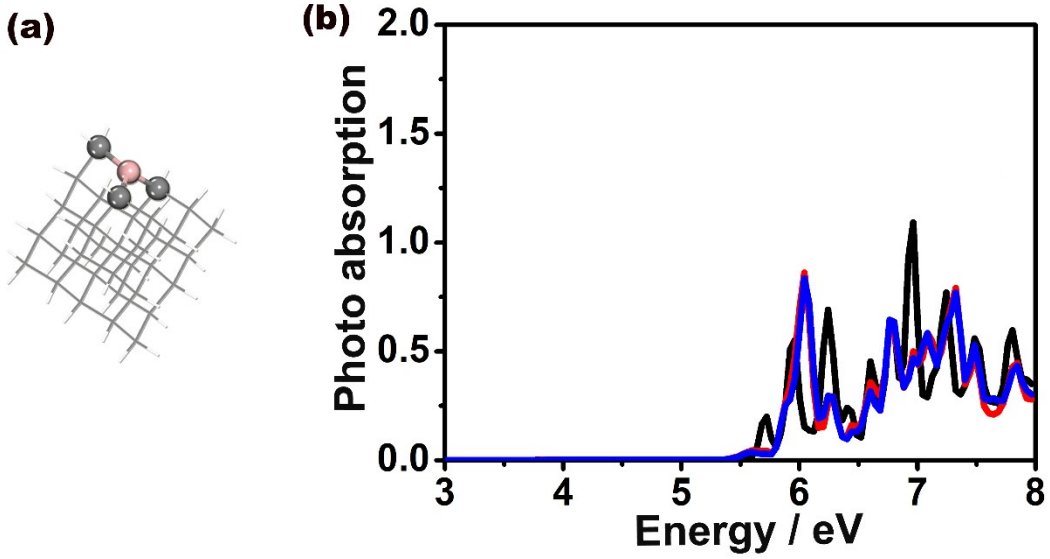

Figure S7. The (a) geometric structure and (b) photoabsorption performance of BDC. The grey, and pink balls in (a) indicate the carbon and boron, respectively. The grey and white lines in (a) denote the carbon and hydrogen, respectively. The black, red and blue lines in (b) denote the light absorption region for the incident light polarized along with the x, y and z directions, respectively.

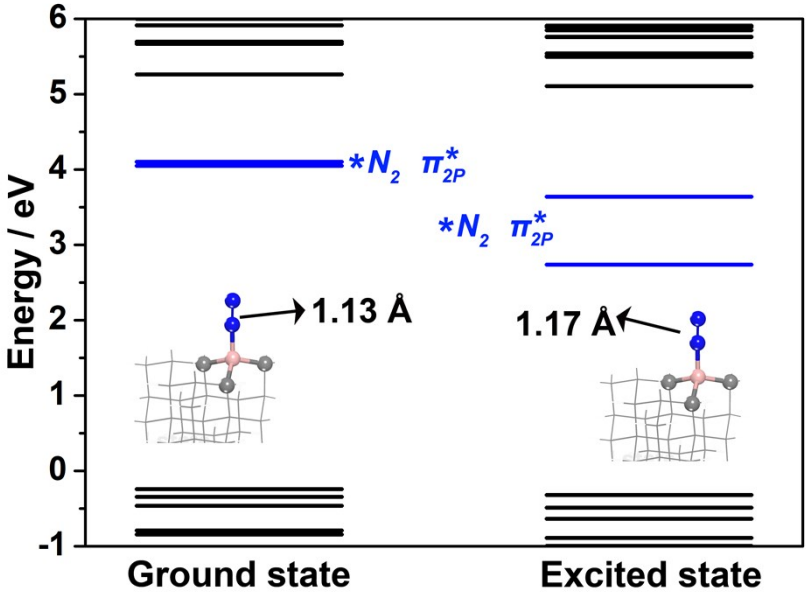

Figure S8. The optimized geometric and electronic structure of ground and excited state N_2 adsorbing on BDC. The Fermi level is set to 0 eV. The blue and black electronic energy level are dominated by *N_2 and BDC, respectively. The grey, pink and blue balls indicate the carbon, boron and nitrogen, respectively. The grey and white line denote the carbon and hydrogen, respectively.

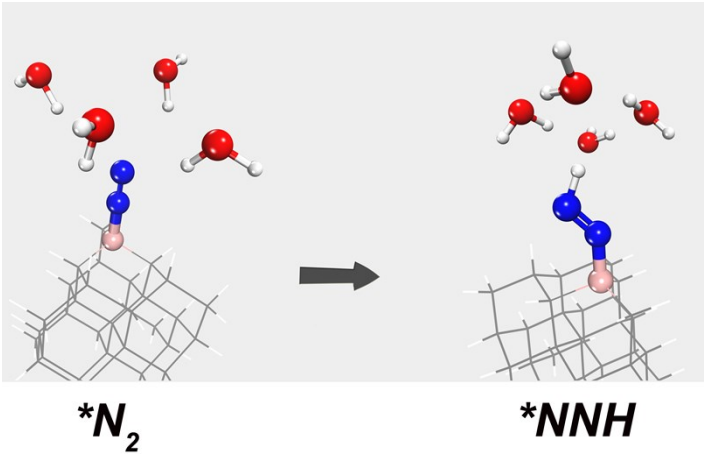

Figure S9. The optimized geometric structure of $*N_2$ and *NNH intermediates with four surrounding H_2O molecules.

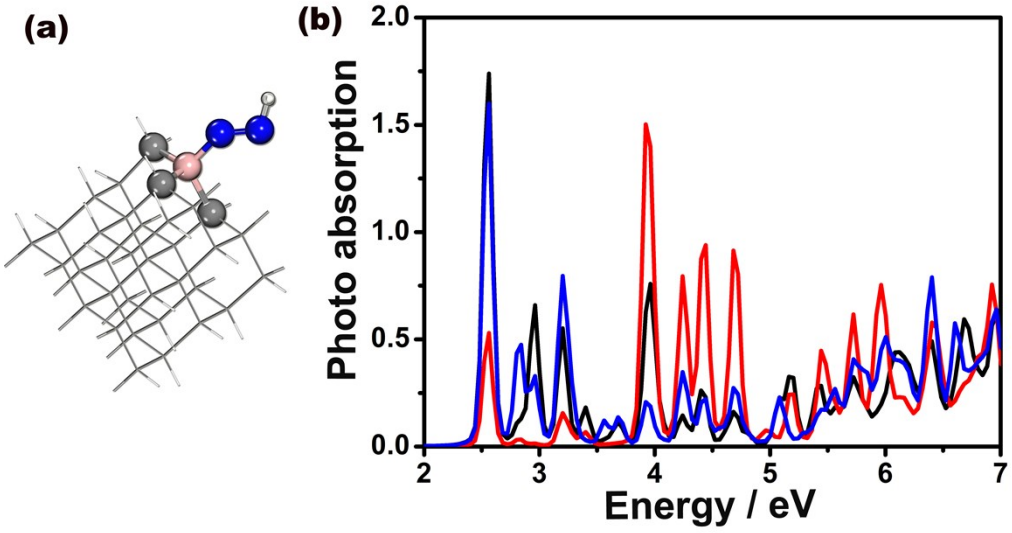

Figure S10. The (a) geometric structure and (b) photoabsorption performance of BDC adsorbing N-NH ligand. The grey, pink, blue and white balls in (a) indicate the carbon, boron, nitrogen and hydrogen, respectively. The grey and white lines in (a) denote the carbon and hydrogen, respectively. The black, red and blue lines in (b) denote the light absorption region for the incident light polarized along with the x, y and z directions, respectively.

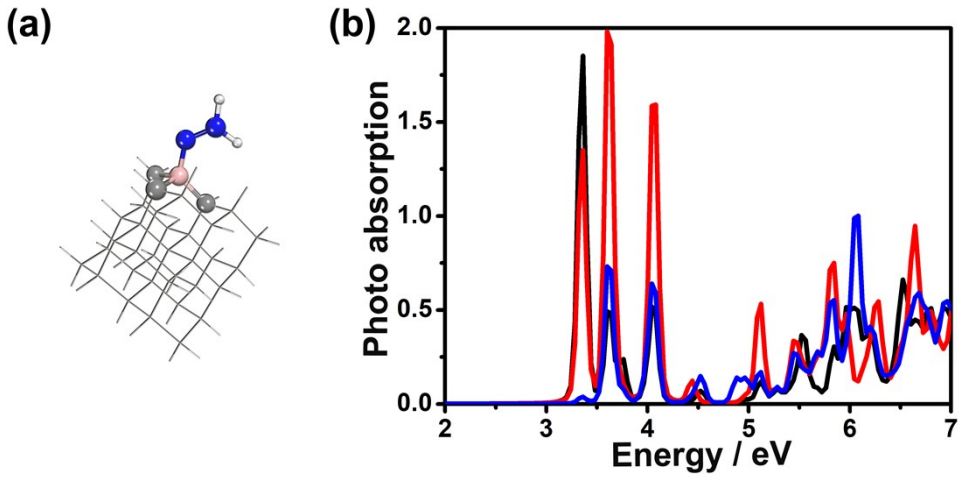

Figure S11. The (a) geometric structure and (b) photoabsorption performance of BDC adsorbing NN-HH ligand. The grey, pink, blue and white balls in (a) indicate the carbon, boron, nitrogen and hydrogen, respectively. The grey and white lines in (a) denote the carbon and hydrogen, respectively. The black, red and blue lines in (b) denote the light absorption region for the incident light polarized along with the x, y and z directions, respectively.

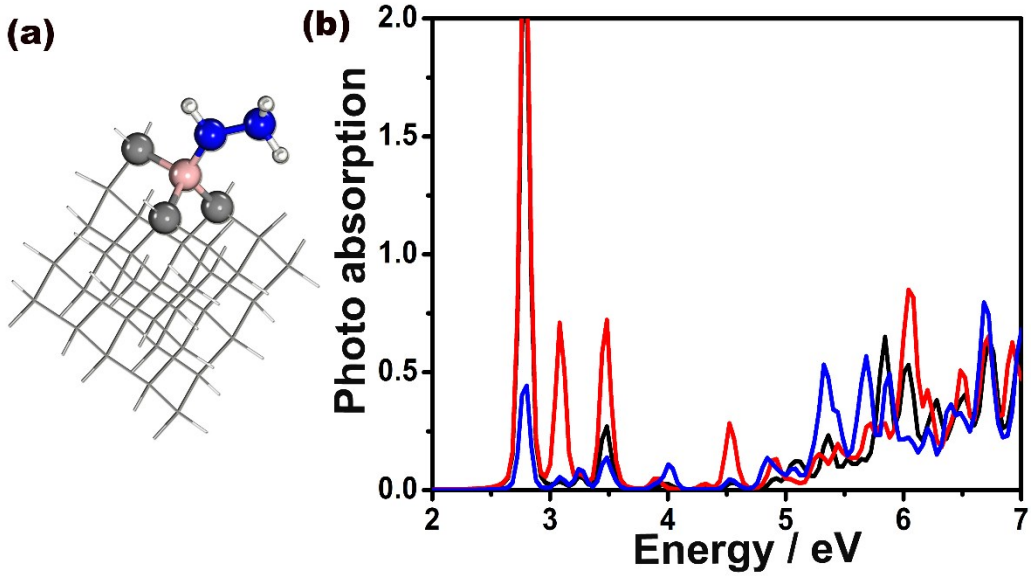

Figure S12. The (a) geometric structure and (b) photoabsorption performance of BDC adsorbing NH-NH_2 ligand. The grey, pink, blue and white balls in (a) indicate the carbon, boron, nitrogen and hydrogen, respectively. The grey and white lines in (a) denote the carbon and hydrogen, respectively. The black, red and blue lines in (b) denote the light absorption region for the incident light polarized along with the x, y and z directions, respectively.

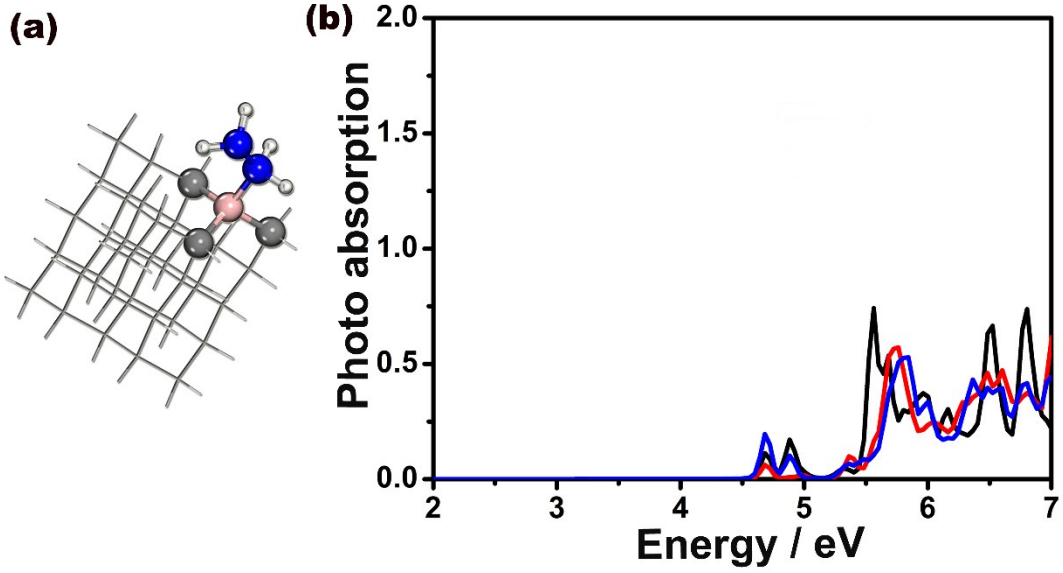

Figure S13. The (a) geometric structure and (b) photoabsorption performance of BDC adsorbing NH_2-NH_2 ligand. The grey, pink, blue and white balls in (a) indicate the carbon, boron, nitrogen and hydrogen, respectively. The grey and white lines in (a) denote the carbon and hydrogen, respectively. The black, red and blue lines in (b) denote the light absorption region for the incident light polarized along with the x, y and z directions, respectively.

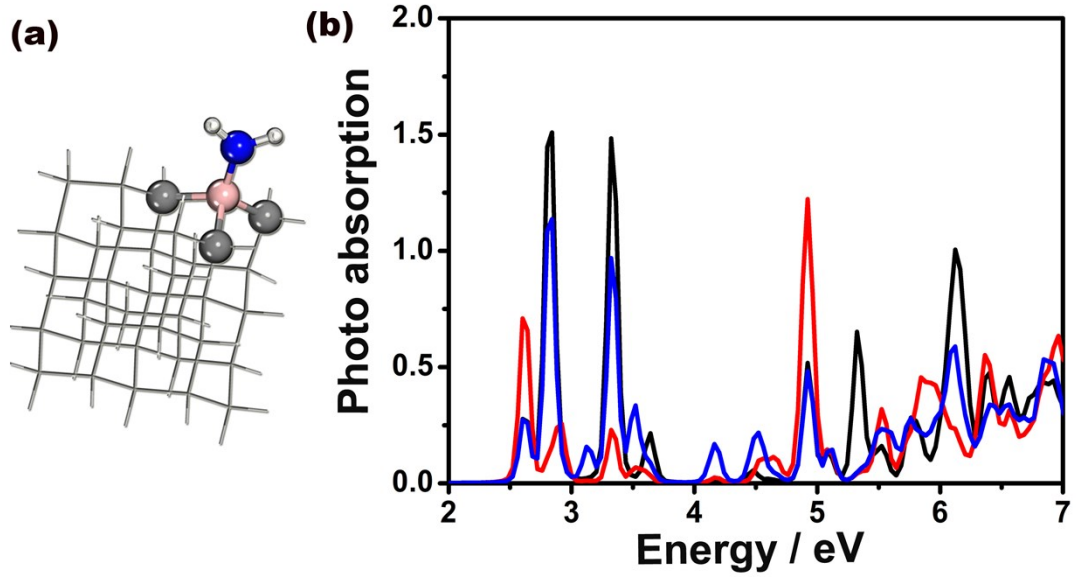

Figure S14. The (a) geometric structure and (b) photoabsorption performance of BDC adsorbing NH_2 ligand. The grey, pink, blue and white balls in (a) indicate the carbon, boron, nitrogen and hydrogen, respectively. The grey and white lines in (a) denote the carbon and hydrogen, respectively. The black, red and blue lines in (b) denote the light absorption region for the incident light polarized along with the x, y and z directions, respectively.

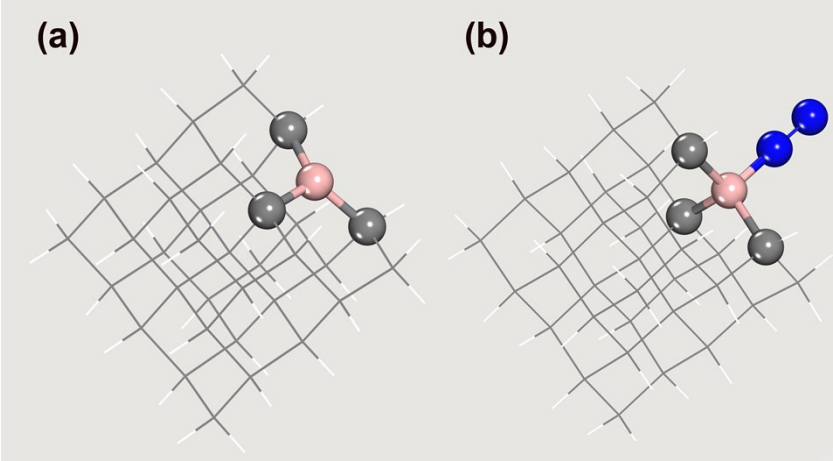

Figure S15. The optimized geometric structure of (a) BDC-2 and (b) N_2 adsorbing on BDC-2. The B doping site is located at the face center of diamond. The grey, pink and blue balls indicate the carbon, boron and nitrogen, respectively. The grey and white line denote the carbon and hydrogen, respectively.

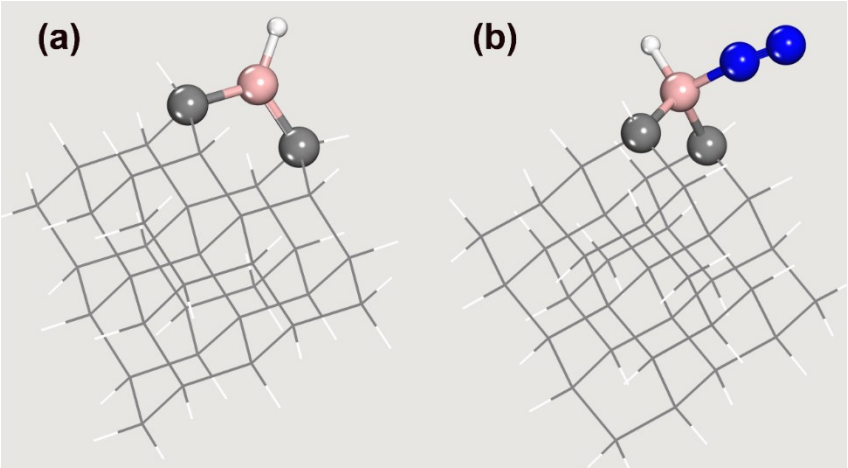

Figure S16. The optimized geometric structure of (a) BDC-3 and (b) N_2 adsorbing on BDC-3. The B doping site is located at the corner of diamond. The B atom is bonded with two C atoms via sp^3 hybridization, and the leaving 2p electron is bonded with hydrogen. This bonding type is similar with B atom bonding with three C atoms. The grey, pink, blue and white balls indicate the carbon, boron, nitrogen and hydrogen, respectively. The grey and white line denote the carbon and hydrogen, respectively.

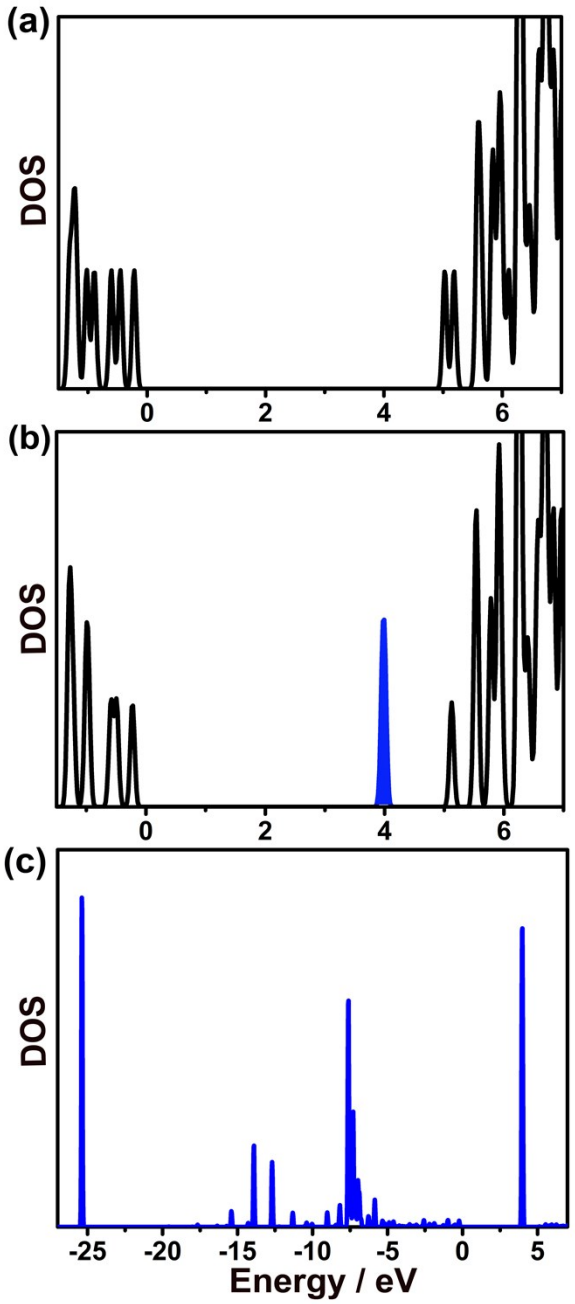

Figure S17. The DOS of (a) BDC-2 and (b) BDC-2 with N_2 adsorption. The blue region in (b) indicates the DOS dominated by the adsorbing N_2. (c) The projected DOS of N_2 for BDC-2 with N_2 adsorption. The Fermi level of BDC-2 is shifted to zero.

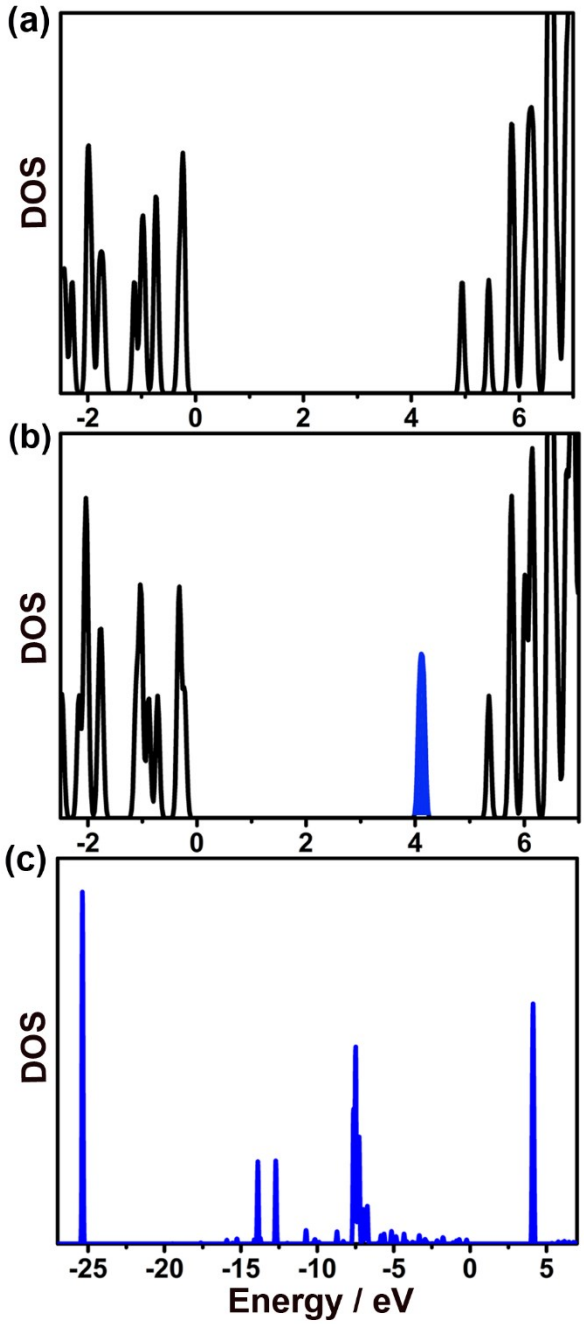

Figure S18. The DOS of (a) BDC-3 and (b) BDC-3 with N_2 adsorption. The blue region in (b) indicates the DOS dominated by the adsorbing N_2. (c) The projected DOS of N_2 for BDC-3 with N_2 adsorption. The Fermi level of BDC-3 is shifted to zero.

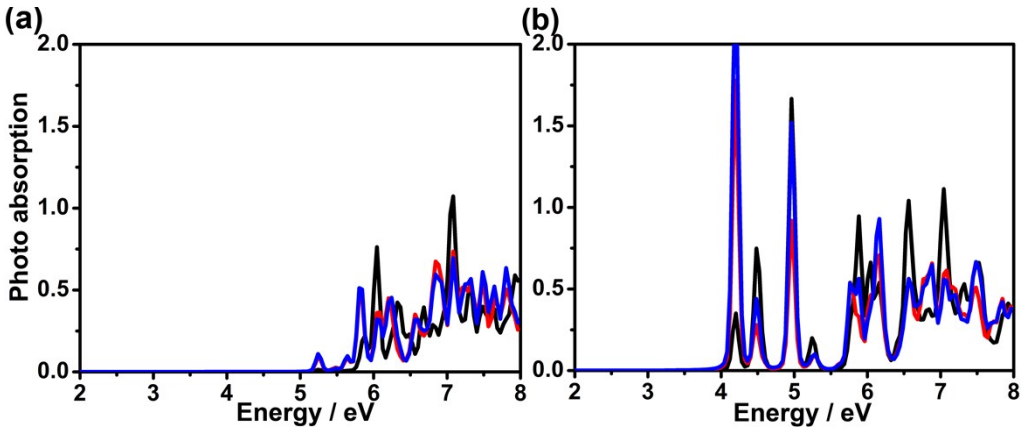

Figure S19. The photoabsorption performance of (a) BDC-2 and (b) BDC-2 adsorbing N_2 ligand. The black, red and blue lines denote the light absorption region for the incident light polarized along with the x, y and z directions, respectively.

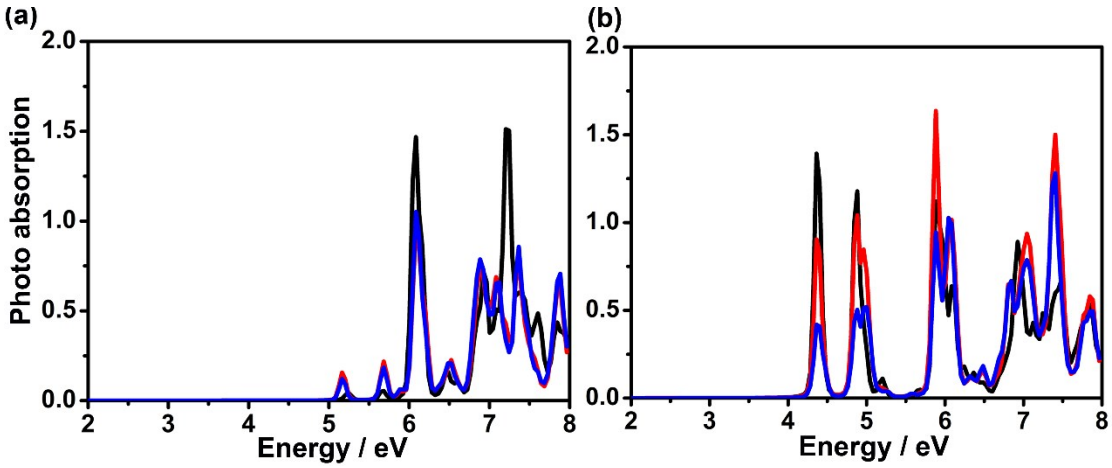

Figure S20. The photoabsorption performance of (a) BDC-3 and (b) BDC-3 adsorbing N_2 ligand. The black, red and blue lines denote the light absorption region for the incident light polarized along with the x, y and z directions, respectively.

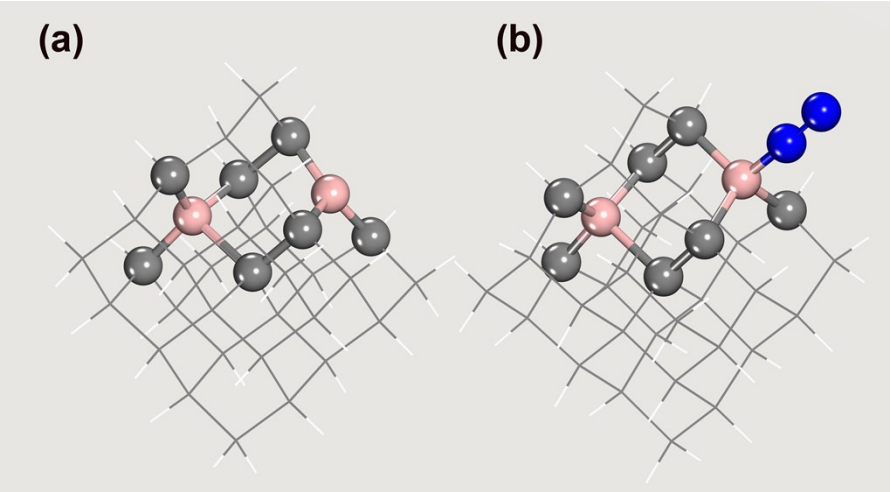

Figure S21. The optimized geometric structure of (a) BDC-4 and (b) N_2 adsorbing on BDC-4. There are two B atoms decorating diamond, one at surface, and the other at near center. The grey, pink and blue balls indicate the carbon, boron and nitrogen, respectively. The grey and white line denote the carbon and hydrogen, respectively.

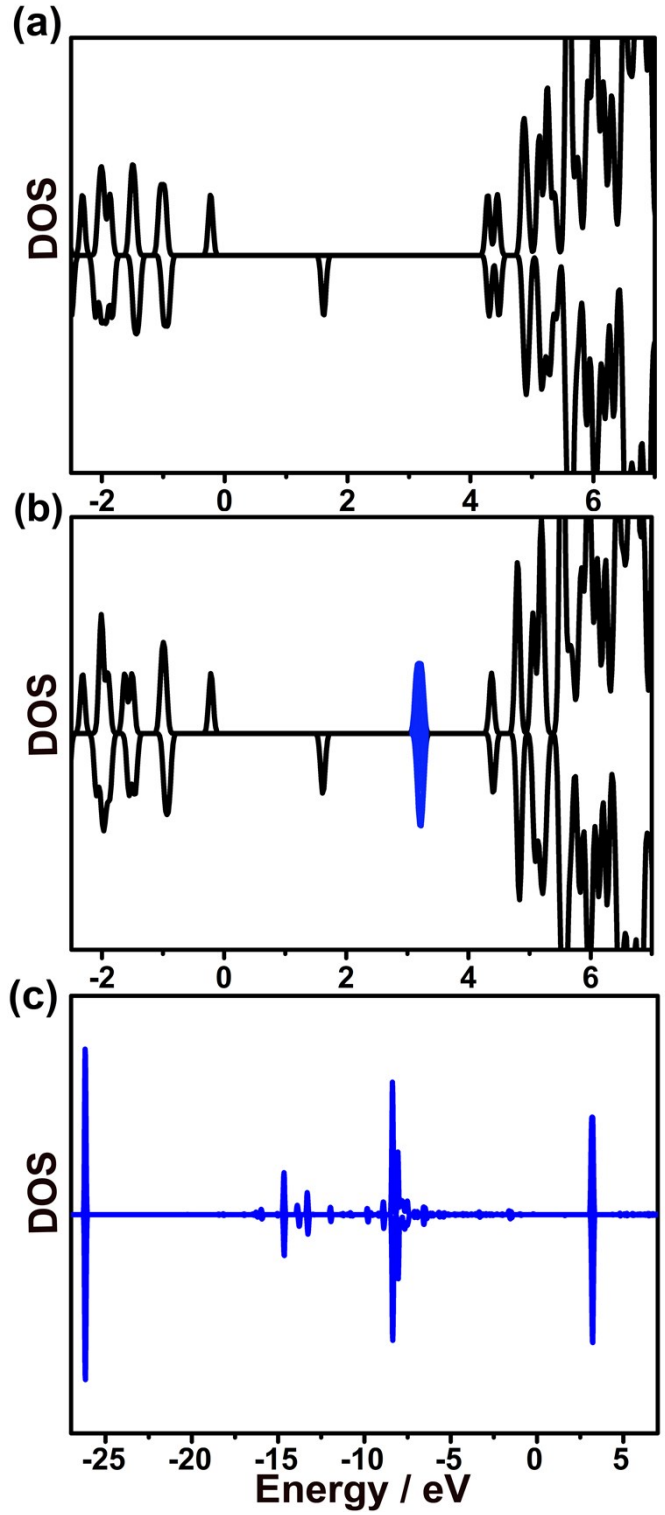

Figure S22. The DOS of (a) BDC-4 and (b) BDC-4 with N_2 adsorption. The blue region in (b) indicates the DOS dominated by the adsorbing N_2. (c) The projected DOS of N_2 for BDC-4 with N_2 adsorption. The Fermi level of BDC-4 is shifted to zero.

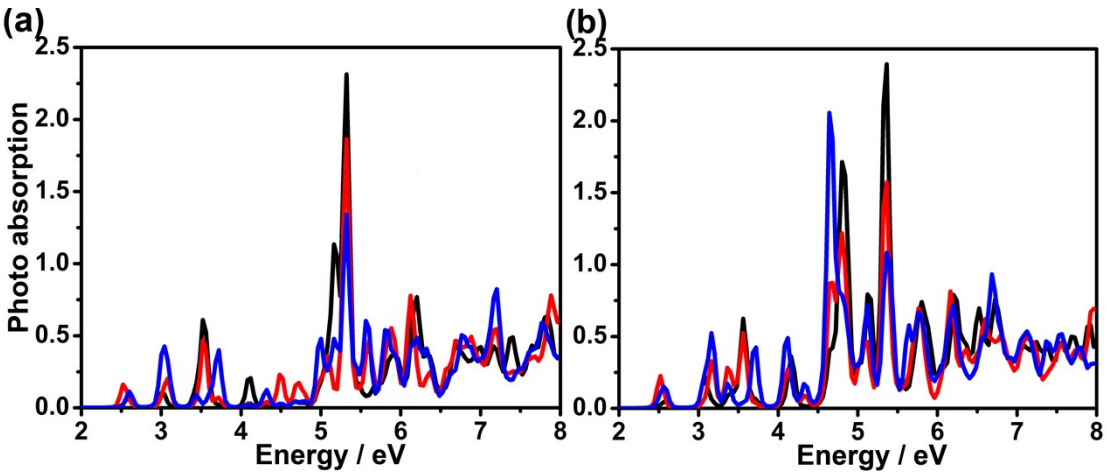

Figure S23. The photoabsorption performance of (a) BDC-4 and (b) BDC-4 adsorbing N_2 ligand. The black, red and blue lines denote the light absorption region for the incident light polarized along with the x, y and z directions, respectively.

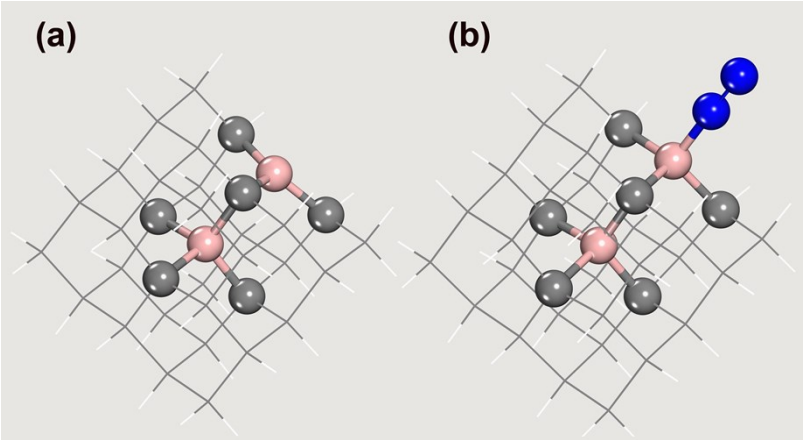

Figure S24. The optimized geometric structure of (a) BDC-5 and (b) N_2 adsorbing on BDC-5. There are two B atoms decorating diamond, one at surface, and the other at center. The grey, pink and blue balls indicate the carbon, boron and nitrogen, respectively. The grey and white line denote the carbon and hydrogen, respectively.

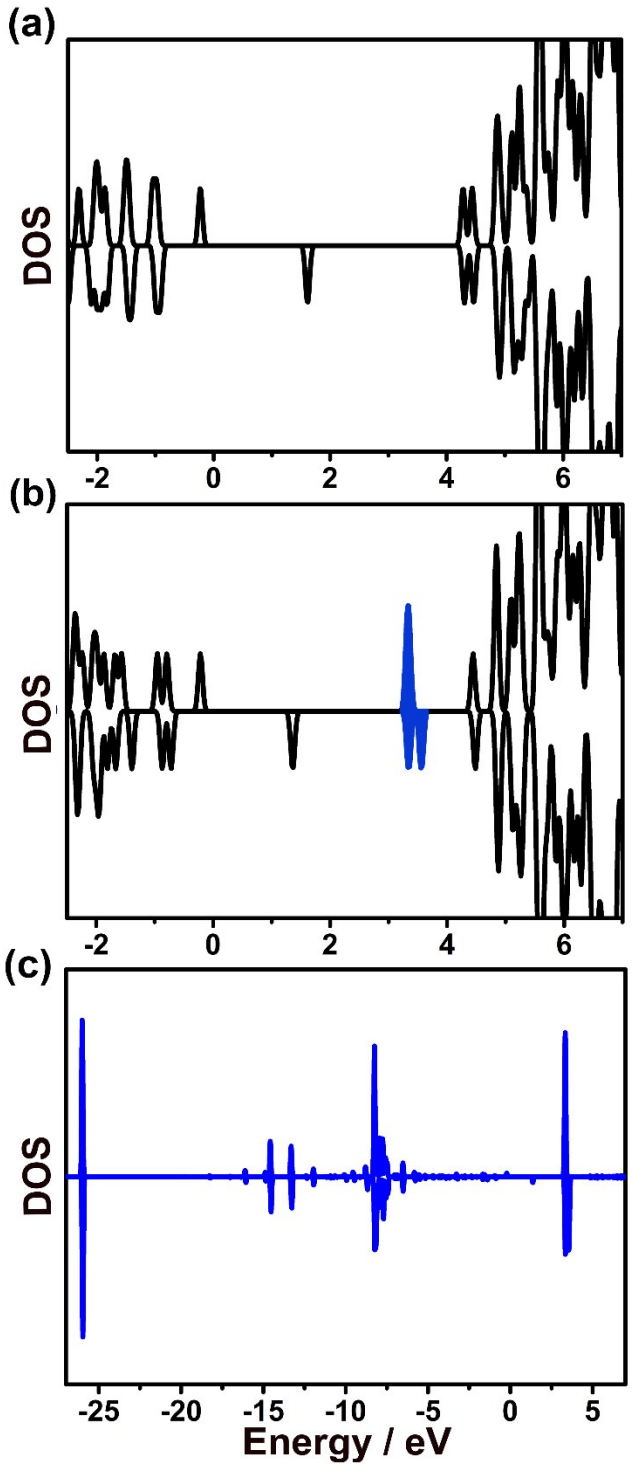

Figure S25. The DOS of (a) BDC-5 and (b) BDC-5 with N_2 adsorption. The blue region in (b) indicates the DOS dominated by the adsorbing N_2. (c) The projected DOS of N_2 for BDC-5 with N_2 adsorption. The Fermi level of BDC-5 is shifted to zero.

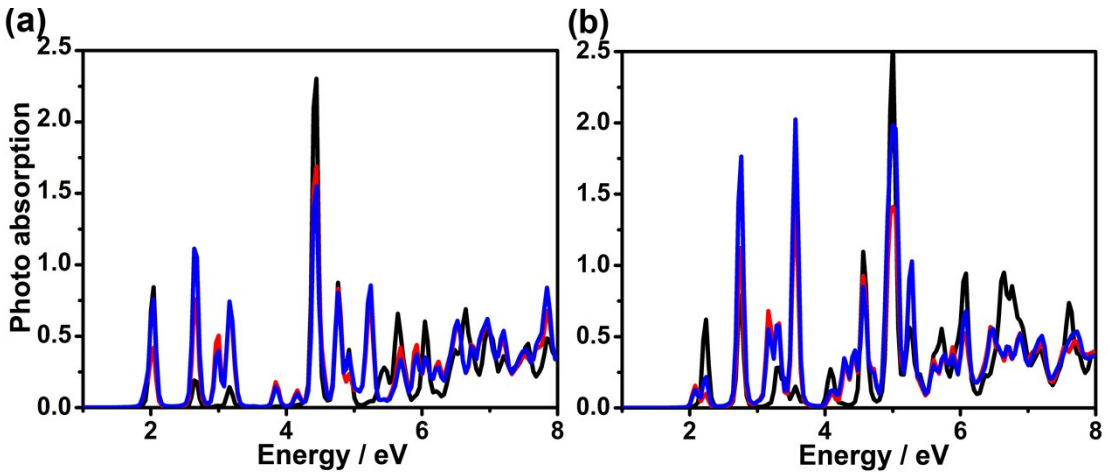

Figure S26. The photoabsorption performance of (a) BDC-5 and (b) BDC-5 adsorbing N_2 ligand. The black, red and blue lines denote the light absorption region for the incident light polarized along with the x, y and z directions, respectively.

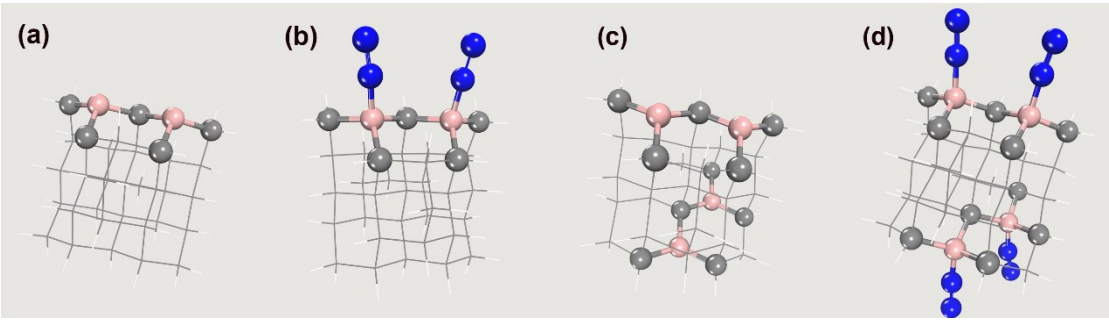

Figure S27. The optimized geometric structure of (a) BDC-6, (b) N_2 adsorbing on BDC-6, (c) BDC-7 and (d) N_2 adsorbing on BDC-7. The grey, pink and blue balls indicate the carbon, boron and nitrogen, respectively. The grey and white line denote the carbon and hydrogen, respectively.

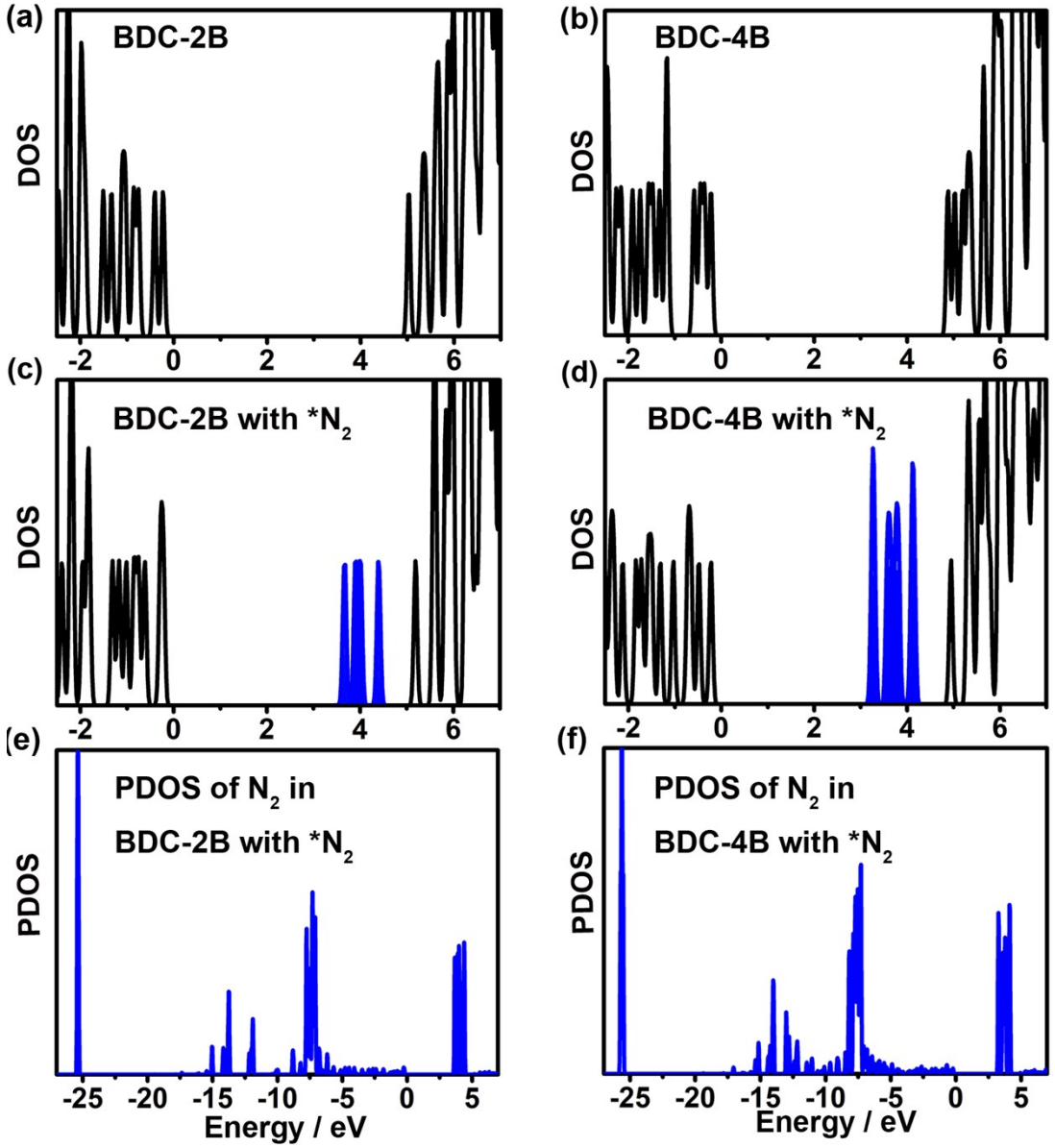

Figure S28. DOS of (a) BDC-6, (b) BDC-7, (c) BDC-6 with N_2 adsorption and (d) BDC-7 with N_2 adsorption. The blue region in (c, d) indicates the DOS dominated by the adsorbing N_2. The projected DOS of N_2 for (e) BDC-2B with N_2 adsorption and (f) BDC-4B with N_2 adsorption. The Fermi level is shifted to zero.

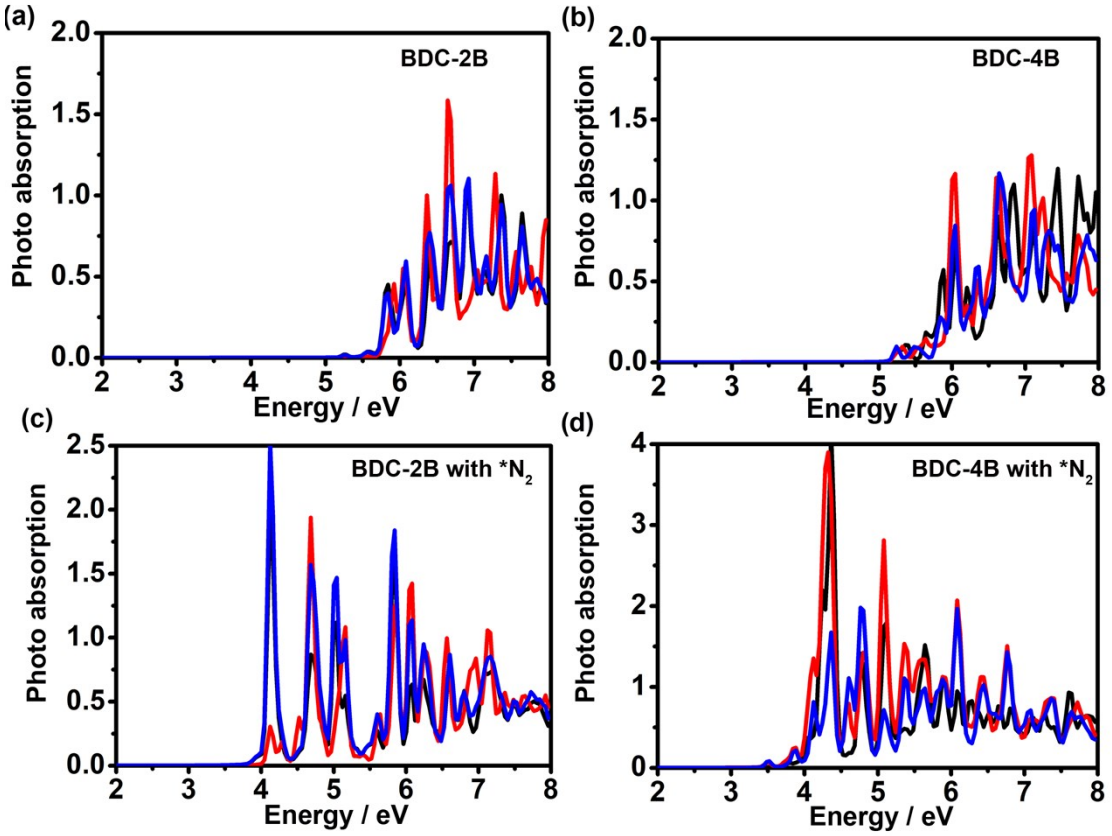

Figure S29. The photoabsorption performance of (a) BDC-6, (b) BDC-7, (c) BDC-6 with N_2 adsorption and (b) BDC-7 with N_2 adsorption. The black, red and blue lines denote the light absorption region for the incident light polarized along with the x, y and z directions, respectively.

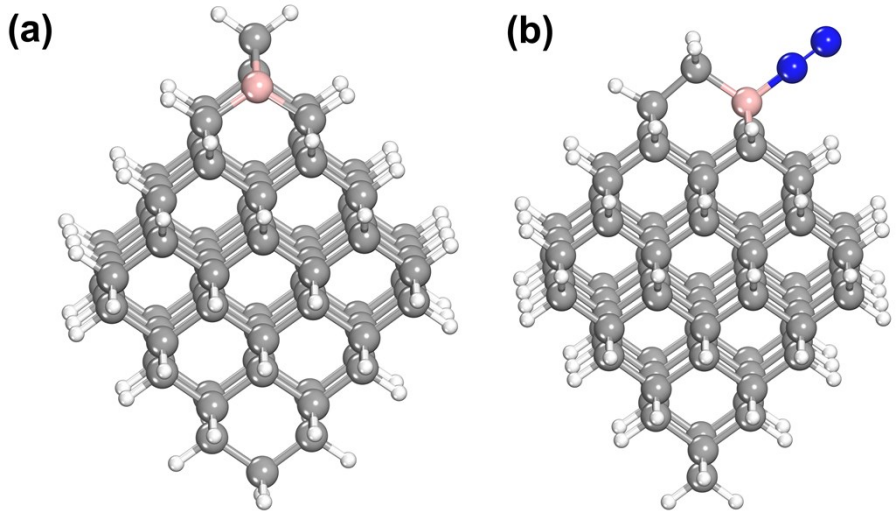

Figure S30. The optimized geometric structure of (a) BDC-8 and (b) N_2 adsorbing on BDC-8. The grey, pink, blue and white balls indicate the carbon, boron, nitrogen and hydrogen, respectively.

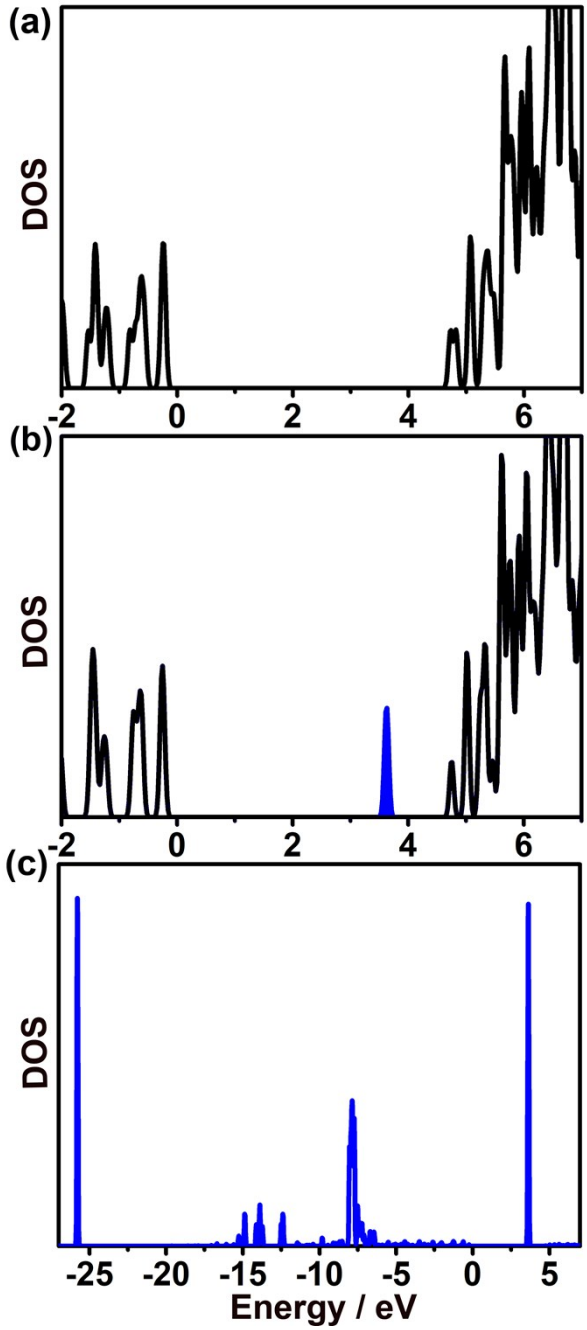

Figure S31. The DOS of (a) BDC-8 and (b) BDC-8 with N_2 adsorption. The blue region in (b) indicates the DOS dominated by the adsorbing N_2. (c) The projected DOS of $*N_2$ for BDC-8 with N_2 adsorption. The Fermi level of BDC-8 is shifted to zero.

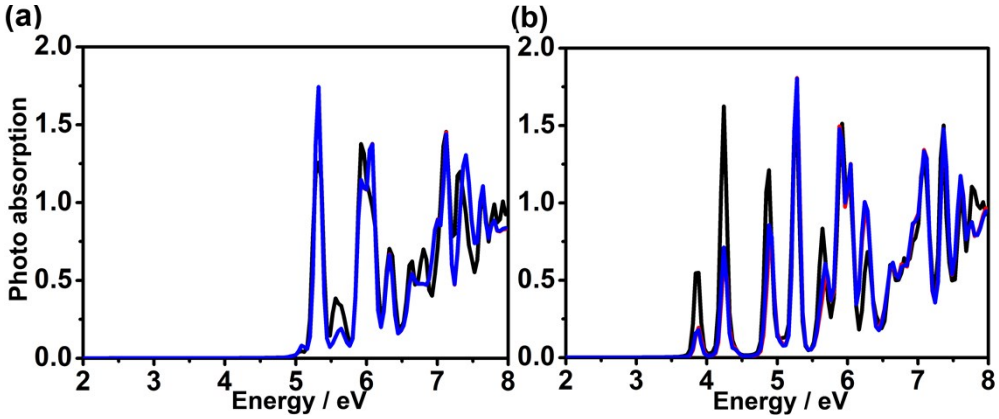

Figure S32. The photoabsorption performance of (a) BDC-9 and (b) BDC-9 adsorbing N_2 ligand. The black, red and blue lines denote the light absorption region for the incident light polarized along with the x, y and z directions, respectively.

References

1 O. V. Prezhdo, *J. Chem. Phys.,* 1999, ***111***, 8366-8377.

2 H. M. Jaeger, S. Fischer and O. V. Prezhdo, *J. Chem. Phys.,* 2012, ***137***, 22A545.

3 P. J. Stephens, F. J. Devlin, C. F. Chabalowski and M. J. Frisch, *J. Phys. Chem.,* 1994, ***98***, 11623-11627.

4 E. V. Lenthe and E. J. Baerends, *J. Comput. Chem.,* 2003, ***24***, 1142-1156.

5 ADF2013 SCM, Theoretical Chemistry; Vrije Universiteit: Amsterdam, the Netherlands. . http://www.scm.com.

6 G. te Velde, F. M. Bickelhaupt, E. J. Baerends, C. Fonseca Guerra, S. J. A. Van Gisbergen, J. G. Snijders and T. Ziegler, *J. Comput. Chem.,* 2001, ***22***, 931-967.

7 C. F. Guerra, J. G. Snijders, G. te Velde and E. J. Baerends, *Theor. Chem. Acc.,* 1998, ***99***, 391-403.

8 A. A. Peterson, F. Abild-Pedersen, F. Studt, J. Rossmeisl and J. K. Nørskov, *Energy Environ. Sci.,* 2010, ***3***, 1311-1315.

9 M. Gajdoš, K. Hummer, G. Kresse, J. Furthmüller and F. Bechstedt, *Phys. Rev. B,* 2006, ***73***, 045112.